

SCIENTIFIC REPORTS



OPEN

A continued fraction based approach for the Two-photon Quantum Rabi Model

Elena Lupo^{1,2}, Anna Napoli^{1,3}, Antonino Messina^{3,4}, Enrique Solano^{5,6,7} & Iñigo L. Egusquiza^{ID}⁸

We study the Two Photon Quantum Rabi Model by way of its spectral functions and survival probabilities. This approach allows numerical precision with large truncation numbers, and thus exploration of the spectral collapse. We provide independent checks and calibration of the numerical results by studying an exactly solvable case and comparing the essential qualitative structure of the spectral functions. We stress that the large time limit of the survival probability provides us with an indicator of spectral collapse, and propose a technique for the detection of this signal in the current and upcoming quantum simulations of the model.

The Quantum Rabi Model (QRM) and the Two-Photon Quantum Rabi Model (2γ QRM) represent two basic models for the description of the interaction of light and matter. The first one describes a two-level system bilinearly coupled to a quantized bosonic field mode; 2γ QRM is one of its simplest generalizations, in which the interaction term is now quadratic in the annihilation and creation bosonic operators. The bilinear QRM for light-matter interaction appeared more than 80 years ago^{1–3}. Yet interest in this model has never waned and, rather, it has even grown recently. This growth mainly stems from its potential application to platforms used for quantum technologies⁴. The QRM depends on two independent parameters, and the dynamical properties of the atom mode are qualitatively very different in different regions of the parameter space. Most of the experimental Cavity Quantum Electrodynamics (CQED) setups are characterized by physical conditions inside the weak-coupling regime, in which the Quantum Rabi model can be effectively simplified to the exactly treatable Jaynes-Cummings model. So as to best describe new, more advanced quantum devices, such as superconducting circuits or trapped ions systems, for instance, the description of the QRM must be extended to the appropriate regions of the parameter space, for which the Jaynes-Cummings approximation fails.

Alternatively, one can view these newer platforms as ‘Quantum Simulators’^{5–7}, in which one can realize models that had been previously discarded as ‘unphysical’. In fact, coupling constant values much higher than the ones typical of CQED setups have been measured in the last years, even reaching the so-called Ultrastrong Coupling (USC, $0.1\omega \ll g \ll \omega$) and the Deep Strong Coupling (DSC, $g \gg \omega$) regimes in the context of circuit Quantum Electrodynamics cQED^{8–10}.

In this vein of Quantum Simulation, other possibilities have appeared. For instance, the interaction Hamiltonian for trapped ions is non-linear, thus allowing this system to be exploited in order to investigate the dynamics of various QRM generalizations^{7,11}. For these reasons, the interest in the QRM and its variants has been rekindled, and a strong effort to construct their solutions and to clarify the relative dynamical properties is under way^{12–18}. A major role in these new developments has been played by the analytic solutions of the QRM, found first in 2011¹⁵ and based on its representation in the Bargmann space of the holomorphic functions¹⁹. Other approaches, exploiting a suitable Bogoliubov transformation¹⁷, or an expansion in the basis of Heun functions, have also been proposed^{20,21}.

Among the many generalizations of the QRM, the Two-photon Quantum Rabi Model (2γ QRM) is of particular interest. It was introduced as an effective model for a three-level system interacting with a bosonic mode in

¹Department of Physics and Chemistry, University of Palermo, Via Archirafi 36, I-90123, Palermo, Italy. ²Advanced Technology Institute and Department of Physics, University of Surrey, Guildford, GU2 7XH, UK. ³I.N.F.N. Sezione di Catania, Catania, Italy. ⁴Department of Mathematics and Computer Science, University of Palermo, Via Archirafi 34, I-90123, Palermo, Italy. ⁵Department of Physical Chemistry, University of the Basque Country UPV/EHU, Apartado 644, 48080, Bilbao, Spain. ⁶IKERBASQUE, Basque Foundation for Science, Maria Diaz de Haro 3, 48013, Bilbao, Spain. ⁷Department of Physics, Shanghai University, 200444, Shanghai, China. ⁸Department of Theoretical Physics and History of Science, University of the Basque Country UPV/EHU, Apartado 644, 48080, Bilbao, Spain. Correspondence and requests for materials should be addressed to E.L. (email: e.lupo@surrey.ac.uk)

which the intermediate level can be adiabatically eliminated^{22–25}. Even if the original phenomenological model was treated in the Rotating Wave Approximation²², some work on the influence of the counter-rotating terms has been carried out in the past^{26–29}. The more recent possibility of realizing the 2 γ QRM in quantum simulators has sparked a new flurry of studies. In particular one should notice the recent proposal for its implementation in trapped ions systems and superconducting circuits^{11,30–32}. Moreover, after Braak's solution for the QRM, the same approach was applied to the determination of the 2 γ QRM spectrum using G-functions^{33,34}. Alternatively the search of the analytic solution has also been presented as an expansion in the generalized squeezed number states^{17,35,36}. An important feature of the model, namely the collapse of the discrete spectrum into a continuum at a value of the coupling constant $g = \omega/2$ ³⁷, has also been made evident both with squeezed states³⁸ and with the Bargmann space¹⁹ approach.

Nonetheless, useful as these analytical approaches are for the spectrum as a function of the coupling strength between the fermionic and bosonic subsystems, an analytical form of the eigenstates, and thus of all quantities of interest, is still to be obtained¹⁸. One such quantity, of particular relevance from an experimental point of view, is the spectral function, defined as $\rho(E, |\Psi\rangle) = \langle \Psi | \delta(E - H) | \Psi \rangle$, in terms of a generic state $|\Psi\rangle$ of the system. In fact $\rho(E, |\Psi\rangle)$ contains all the information useful for generating the time evolution of $|\Psi\rangle$, namely those eigenvalues of the Hamiltonian whose eigenfunctions have an overlap with $|\Psi\rangle$ and the relative transition probabilities.

In this paper we put forward the spectral analysis of a factorized state $|n, \sigma\rangle \equiv |n\rangle|\sigma\rangle$ of the 2 γ QRM, n being the eigenvalue of the number operator $a^\dagger a$ and σ being the eigenvalue of the spin operator σ_z . This approach, valid in each point of the parameter space, is an alternative to the Bargmann solution of the model. To achieve this goal the relevant matrix element of the resolvent is presented in continued fraction form. We have thus direct access to two complementary quantities of interest: the spectral density and the survival probability. The structure of our approach allows us clean access to the dynamics of the system near the collapse point of the 2 γ QRM corresponding to the value of $g = 0.5\omega$.

The paper is organized as follows: we present the model and apply a unitary transformation such that the eigenstates factorize in a bosonic and a spin part³⁹; then we exploit the connection between the resolvent of a tridiagonal matrix and continued fractions to obtain a numerical determination for the spectral function of factorized states $|n, \sigma\rangle$; finally we use the previous results to study the survival probability of the vacuum state of the system.

The two-photon model

The Two-photon Quantum Rabi Model (2 γ QRM) presents an interaction which is non linear in the bosonic operators. The Hamiltonian can be expressed as:

$$H = \omega a^\dagger a + \frac{\omega_0}{2} \sigma_z + g(a^2 + (a^\dagger)^2) \sigma_x \quad (1)$$

where ω is the frequency of the bosonic mode, ω_0 the atomic frequency and g the coupling constant between the two subsystems. Here and subsequently we set \hbar to 1. The spectrum of this model has been numerically calculated in many works^{11,17,27,33–37}, and a link with the squeezed number states has been pointed out^{17,35,36}. This link provides us with a better understanding of the spectrum collapse at $g = \omega/2$ ^{11,37}, as follows. Define, as usual, the squeezing operator $S(\beta) = e^{-\frac{\beta}{2}(a^2 - (a^\dagger)^2)}$, and consider the 2 γ QRM for $\omega_0 = 0$, written in the basis for which σ_x is diagonal. Under squeezing transformations with squeezing parameters $\beta_\pm = \pm \frac{1}{2} \tanh^{-1} \left(\frac{2g}{\omega} \right)$ one of the diagonal elements of the Hamiltonian becomes a harmonic oscillator. Clearly, the limit $|g| \rightarrow \omega/2$ is the limit of infinite squeezing. This entails, in what regards the spectrum, the collapse of eigenvalues into a continuum in the limit $g \rightarrow 0.5\omega$, and the (generalized) eigenstates are no longer normalizable^{11,37}. As in¹¹, one can rewrite the Hamiltonian (1) in terms of the position and momentum operators of the oscillator, $x = \sqrt{\frac{1}{2\omega}}(a + a^\dagger)$ and $p = i\sqrt{\frac{\omega}{2}}(a^\dagger - a)$, with unit mass:

$$H = \frac{\omega}{2} \left\{ (\omega - 2g\sigma_x) \frac{p^2}{\omega^2} + (\omega + 2g\sigma_x) x^2 \right\} + \frac{\omega_0}{2} \sigma_z - \frac{\omega}{2} \quad (2)$$

For $g < \omega/2$ the effective potential makes the system stable, while at the point $g = \omega/2$ one of the two quantities x^2 or p^2 disappears and the spectrum collapses into a continuum. This is immediately obvious if $\omega_0 = 0$. Were this parameter different from zero, isolated eigenstates would appear. In the context of an analysis of the asymptotic behaviour of solutions in Bargmann space, the collapse point coincides with the limit situation, for which the eigenfunction is no longer normalizable^{11,16,37}.

As is well known, the QRM Hamiltonian commutes with a parity operator, and its eigenvalues can be arranged in parity subspaces. In the case of the 2 γ QRM the symmetry is \mathbb{Z}_4 , since the Hamiltonian commutes with $\Pi_4 = -e^{i\frac{\pi}{2}a^\dagger a} \sigma_z$, whose eigenvalues are the quartic roots of unity $\{\pm 1, \pm i\}$. It follows that the full Hilbert space is organized in four infinite-dimensional chains:

$$\begin{aligned} |0, -\rangle &\leftrightarrow |2, +\rangle \leftrightarrow |4, -\rangle \leftrightarrow |6, +\rangle \leftrightarrow |8, -\rangle \leftrightarrow \dots \\ |1, +\rangle &\leftrightarrow |3, -\rangle \leftrightarrow |5, +\rangle \leftrightarrow |7, -\rangle \leftrightarrow |9, +\rangle \leftrightarrow \dots \\ |0, +\rangle &\leftrightarrow |2, -\rangle \leftrightarrow |4, +\rangle \leftrightarrow |6, -\rangle \leftrightarrow |8, +\rangle \leftrightarrow \dots \\ |1, -\rangle &\leftrightarrow |3, +\rangle \leftrightarrow |5, -\rangle \leftrightarrow |7, +\rangle \leftrightarrow |9, -\rangle \leftrightarrow \dots \end{aligned} \quad (3)$$

We denote the corresponding four infinite-dimensional subspaces S_w , with $w \in \{\pm 1, \pm i\}$. For instance, the vacuum state $|0, - \rangle \equiv |0\rangle| - 1\rangle$ belongs to the subspace S_{+1} . Explicitly,

$$|\Psi_w\rangle = \sum_{n=0}^{\infty} a_n |2n, \sigma = - w \cos(\pi n)\rangle, \quad \text{for } w = \pm 1; \tag{4a}$$

$$|\Psi_w\rangle = \sum_{n=0}^{\infty} a_n |2n + 1, \sigma = - iw \cos(\pi n)\rangle, \quad \text{for } w = \pm i. \tag{4b}$$

We shall now apply a transformation which factorizes the state $|\Psi_w\rangle$ into a bosonic and an atomic part, following the procedure of³⁹ for the QRM. In other words¹², we use the parity basis. This factorization is indeed achieved with the rotation

$$T = e^{-i\frac{\pi}{4}(\sigma_x - 1)a^\dagger a} = \frac{1}{2}(1 - \sigma_x)e^{i\frac{\pi}{2}a^\dagger a} + \frac{1}{2}(1 + \sigma_x). \tag{5}$$

This rotation transforms the Hamiltonian into $\tilde{H} = T^\dagger H T$, explicitly

$$\tilde{H} = \omega a^\dagger a + \frac{\omega_0}{2} \cos\left(\frac{\pi}{2} a^\dagger a\right) \sigma_z + \frac{\omega_0}{2} \sin\left(\frac{\pi}{2} a^\dagger a\right) \sigma_y + g((a^2) + (a^\dagger)^2). \tag{6}$$

The coupling term is now expressed as diagonal in the bosonic number operator. Under this rotation the subspaces of constant 4-parity become:

$$\begin{aligned} \tilde{S}_{-1} &= \{T^\dagger|0, + \rangle, T^\dagger|2, - \rangle, \dots\} \equiv \{|2n, + \rangle, n \in \mathbb{N}\} \\ \tilde{S}_{+1} &= \{T^\dagger|0, - \rangle, T^\dagger|2, + \rangle, \dots\} \equiv \{|2n, - \rangle, n \in \mathbb{N}\} \\ \tilde{S}_{-i} &= \{T^\dagger|1, - \rangle, T^\dagger|3, + \rangle, \dots\} \equiv \{|2n + 1\rangle \otimes \frac{1}{\sqrt{2}}(| + \rangle + i| - \rangle), n \in \mathbb{N}\} \\ \tilde{S}_{+i} &= \{T^\dagger|1, + \rangle, T^\dagger|3, - \rangle, \dots\} \equiv \{|2n + 1\rangle \otimes \frac{1}{\sqrt{2}}(| + \rangle - i| - \rangle), n \in \mathbb{N}\} \end{aligned} \tag{7}$$

and the Hamiltonian projected into each subspace is a quadratic of the bosonic creation and annihilation operators,

$$\begin{aligned} \tilde{H}_{\pm 1} &= \omega a^\dagger a + g(a^2 + (a^\dagger)^2) \mp \frac{1}{2}\omega_0 \cos\left(\frac{a^\dagger a}{2}\pi\right) \\ \tilde{H}_{\pm i} &= \omega a^\dagger a + g(a^2 + (a^\dagger)^2) \mp \frac{1}{2}\omega_0 \cos\left(\frac{a^\dagger a - 1}{2}\pi\right). \end{aligned} \tag{8}$$

Thus each effective Hamiltonian \tilde{H}_w is explicitly tridiagonal in the Fock basis.

The Spectral Function and the Resolvent

In this section we derive an expression of the spectral function of a factorised state $|n, \sigma\rangle$ in a continued fraction form. The spectral function $\rho(E, |\Psi\rangle, |\Psi'\rangle)$ is the matrix element $\rho(E)_{\Psi, \Psi'}$ of the microcanonical density operator defined in the following way:

$$\rho(E) = \delta(E - H) = \sum_{\lambda} |\varepsilon_{\lambda}\rangle \langle \varepsilon_{\lambda}| \delta(E - E_{\lambda}) \tag{9}$$

where H is the Hamiltonian of the model and $|\varepsilon_{\lambda}\rangle$ is the eigenstate of H related to the eigenvalue $E_{\lambda}, H|\varepsilon_{\lambda}\rangle = E_{\lambda}|\varepsilon_{\lambda}\rangle$. Other than in quantum statistical mechanics, it appears in relation with the resolvent $(E - H)^{-1}$, whose spectral representation is:

$$R_H(E) = \frac{1}{E - H} = \sum_{\lambda} \frac{|\varepsilon_{\lambda}\rangle \langle \varepsilon_{\lambda}|}{E - E_{\lambda}} = \lim_{\varepsilon \rightarrow 0^+} \int_{-\infty}^{+\infty} \frac{1}{E - E' - i\varepsilon} \rho(E') dE' \tag{10}$$

From the definition (9) one can see that the diagonal element $\rho(E, |\Psi\rangle)$ contains all the spectral information useful in the study of the state $|\Psi\rangle$ of the system. It can be in fact interpreted as the probability distribution of the state $|\Psi\rangle$ to be in a particular eigenstate of the Hamiltonian:

$$\rho(E, |\Psi\rangle) = \sum_{\lambda} |\langle \varepsilon_{\lambda} | \Psi \rangle|^2 \delta(E - E_{\lambda}), \tag{11}$$

and it is instrumental in studying the time evolution of the state.

Its numerical computation can be rather involved if attacked in terms of Bargmann functions, though. Here we address this issue by making use of the connection of the spectral function to the resolvent of the system. The distributional identities $\lim_{\varepsilon \rightarrow 0} \frac{1}{x \pm i\varepsilon} = \mathcal{P} \frac{1}{x} \mp i\pi \delta(x)$, with $\varepsilon > 0$ and \mathcal{P} principal part, determine

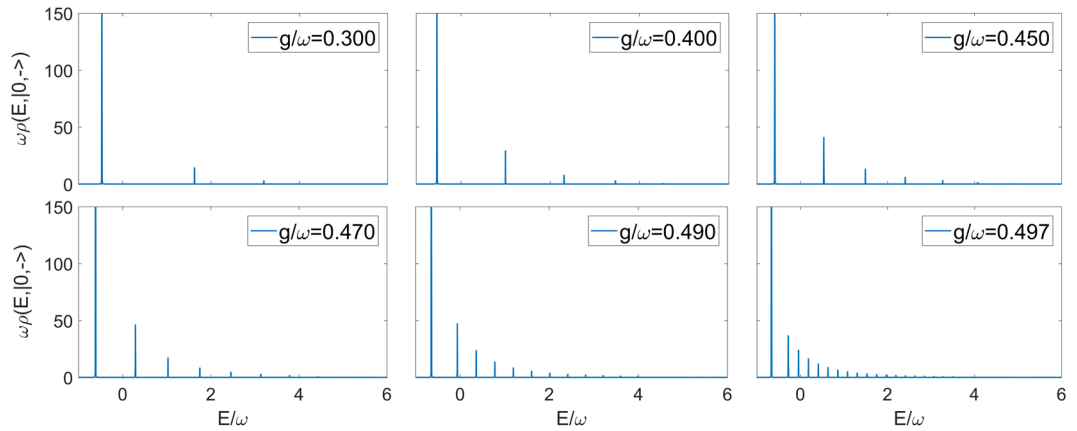


Figure 1. Spectral density related to the state $|0, -\rangle$ of the 2γ QRM at different values of g/ω . The value of the atomic frequency is $\omega_0 = 0.8\omega$ in all cases, while $\varepsilon = 0.0005$ (see Eq. (12)). The truncation of the continued fraction is chosen in order to have convergence.

$$\rho(E, |\Psi\rangle) = \frac{1}{\pi} \lim_{\varepsilon \rightarrow 0} \text{Im} \langle \Psi | (E - H - i\varepsilon)^{-1} | \Psi \rangle. \tag{12}$$

In the factorized states basis $|n, \sigma\rangle$, the resolvent of the QRM and 2γ QRM can readily be expressed in continued fraction form (see^{40,41} or Appendix A), which makes a numerical calculation of the spectral function $\rho(E, |n, \sigma\rangle)$ accessible. Notice that the use of continued fractions has been a staple in the treatment of the QRM, in different guises and forms⁴². Taking the rotated Hamiltonian (6), the element of the resolvent related to the state $|n, \sigma\rangle$ is in the form:

$$\langle n, \sigma | TR_{\tilde{H}} T^\dagger | n, \sigma \rangle = \frac{1}{(z - A_{[\frac{n}{2}]}) - \frac{R_{[\frac{n}{2}]+1}^2}{(z - A_{[\frac{n}{2}]+1}) - \frac{R_{[\frac{n}{2}]+2}^2}{\dots}} - \frac{R_{[\frac{n}{2}] }^2}{(z - A_{[\frac{n}{2}]-1}) - \frac{R_{[\frac{n}{2}]-1}^2}{z - A_0}}} \tag{13}$$

where we set $z = E - i\varepsilon$ for the numerical calculation of (12) and the coefficients A_j and R_j depend on the subspace which $|n, \sigma\rangle$ belongs to: if the state has the form $|2n, \pm (-1)^n\rangle$ (i.e. it belongs to the subspace $S_{\mp 1}$) the coefficients are $A_j = 2j\omega \pm (-1)^j \omega_0/2$ and $R_j = g\sqrt{2j(2j-1)}$; if the state is in the form $|2n+1, \pm (-1)^n\rangle$ (i.e. it belongs to the subspace $S_{\pm 1}$) the coefficients are $A_j = (2j+1)\omega \mp (-1)^j \omega_0/2$ and $R_j = g\sqrt{2j(2j+1)}$.

Equation (13) allows us to calculate the spectral function of any factorized state $|n, \sigma\rangle$ of the 2γ QRM. In this work we show the results related to the positive parity subspace S_{+1} . Since we are working in the rotated basis, from now on we use $|2n, -\rangle$ as notation for the state belonging to \tilde{S}_{+1} .

The convergence of the continued fraction has been determined through Pringsheim’s Theorem, under the condition that $g < \omega/2$ (see Appendix B). The actual computation of the continued fraction expansion involves a truncation in Fock space for each truncation of the continued fraction. In Fig. 1 we report the numerical determination of the spectral density for the vacuum state of the 2γ QRM at different values of g/ω . Notice that the parameter ε has to be fixed for the numerical evaluation. Its value is chosen in such a way it doesn’t affect the ratio between the peaks, and a smaller value would result only in a common scaling factor that does not bring improvement in the determination of the spectral function.

The method at hand, namely the numerical computation by continued fractions of spectral functions, allows us to insert much higher truncation numbers than with a direct simulation with truncation in Fock space, even very close to the collapse point $g/\omega = 0.5$, where the spectrum will no longer be purely discrete. Fig. 2 shows the spectral density as we approach the special value $g/\omega = 0.5$, making apparent this change of the spectrum into an isolated discrete value and a continuum.

We now apply our technique to the collapse point $g/\omega = 0.5$, even though Pringsheim’s theorem only guarantees convergence in the discrete case $g/\omega < 0.5$. In fact the continued fraction approach allows only a discrete approximation of a continuum spectrum, but this is done at very high truncation numbers. In Fig. 3 the spectral function of the vacuum state for $g/\omega = 0.5$ is calculated at different values of ω_0 . A first point of note is that the presence of an isolated ground state is linked to the atomic frequency ω_0 being different from zero. Secondly, observe that the energy difference between the ground state and the continuum (Fig. 4) is not linear in ω_0 , as observed also for $g/\omega < 0.5$ in previous papers^{33,34,37}.

In the case $\omega_0 = 0$ the spectral function $\rho_0(E, |2n, -\rangle)$, with $|2n, -\rangle \in \tilde{S}_{+1}$, can be calculated analytically. Consider the Hamiltonian of the 2γ QRM projected in \tilde{S}_{+1} for a coupling value $g = \omega/2$:

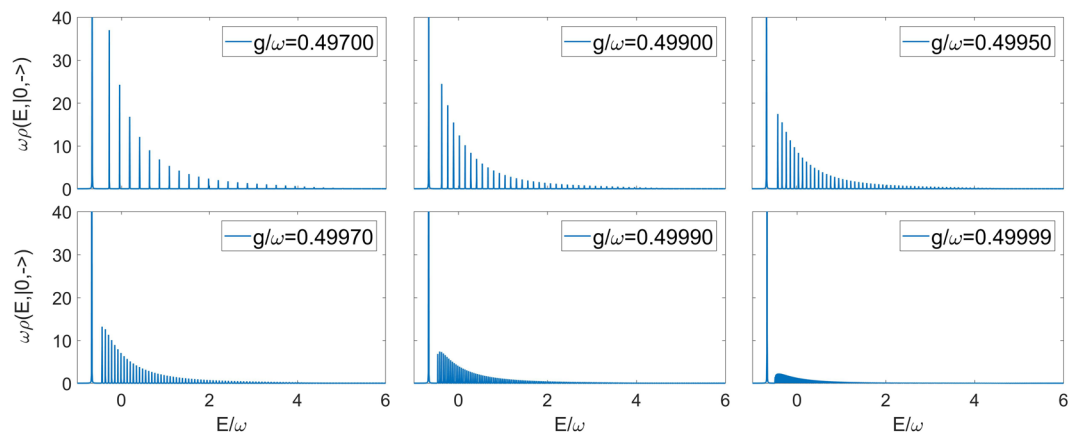


Figure 2. Spectral density related to the state $|0, -\rangle$ of the 2γ QRM at different values of g/ω , close to the collapse point $g/\omega = 0.5$. The value of the atomic frequency is $\omega_0 = 0.8\omega$ in all cases, while $\varepsilon = 0.0005$ (see Eq. (12)). The truncation of the continued fraction is chosen in order to have convergence.

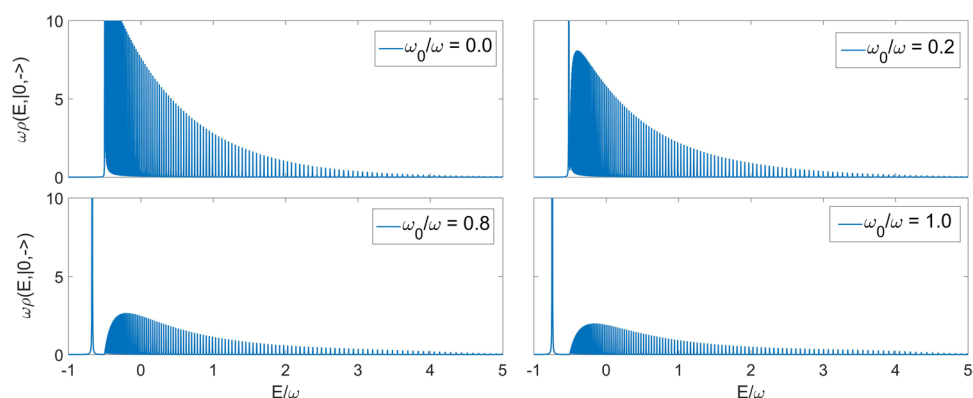


Figure 3. Spectral function related to the vacuum state $|0, -\rangle$ of the 2γ QRM in correspondence of the collapse point $g/\omega = 0.5$, at different values of ω_0 . It can be seen that the position of the isolated ground state is dependent on the value of the atomic frequency. In all cases $\varepsilon = 0.0005$ (see Eq. (12)), while the truncation number exploited for the continued fraction is $N = 8000$.

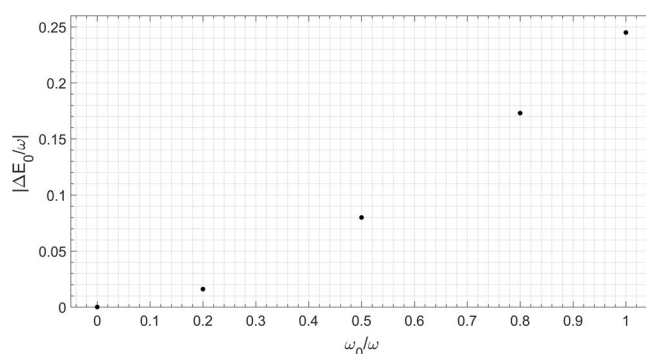


Figure 4. Energy difference between the ground state and the continuum part of the spectrum in varying the two-level parameter ω_0 .

$$\tilde{H}_\pm = \omega a^\dagger a + \frac{\omega}{2}(a^2 + (a^\dagger)^2) - \frac{\omega_0}{2}(-1)^{a^\dagger a/2} \tag{14}$$

We can express it in terms of x and p operators. In fact, knowing that $a = \sqrt{\frac{\omega}{2}}(x + ip/\omega)$ and $a^\dagger = \sqrt{\frac{\omega}{2}}(x - ip/\omega)$, we obtain:

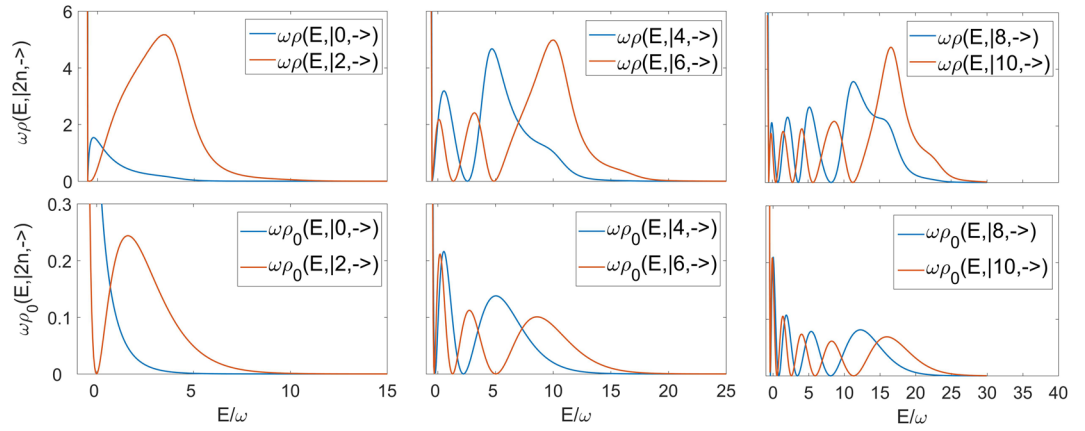


Figure 5. Comparison between the the spectral functions related to the first six states belonging to \tilde{S}_{+1} , between the cases $\omega_0 = 0.8\omega$ and $\omega_0 = 0$ (whose analytic form is known) at the collapse point $g/\omega = 0.5$. In all cases $\varepsilon = 0.0005$, while the truncation number exploited for the continued fraction is $N = 24000$.

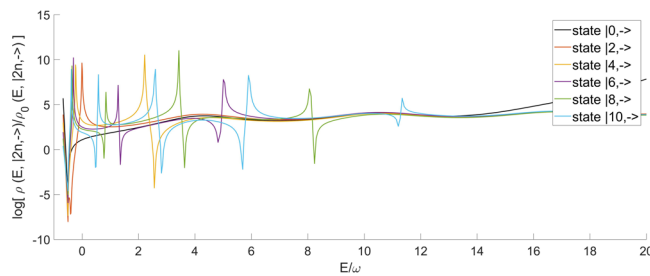


Figure 6. Plot of the ratio between the two cases compared in Fig. 5. It can be seen that for high energies the ratio between the spectral function in the case $\omega_0 \neq 0$ and the exact case $\omega_0 = 0$ is constant.

$$\tilde{H}_{\pm} = \omega^2 x^2 - \frac{\omega}{2} - \frac{\omega_0}{2} (-1)^{(x^2+p^2-1)/4} \tag{15}$$

In the case $\omega_0 = 0$ the Schrödinger equation takes the form $(\omega^2 x^2 - \omega/2)|\Psi(x)\rangle = E|\Psi(x)\rangle$ and the eigenstates coincide with the position operator eigenstates $|x\rangle$. Therefore, the spectral function related to the state $|2n, -\rangle$ can be expressed in terms of the Hermite polynomials $H_m(\xi)$:

$$\rho_0(E, |2n, -\rangle) = \frac{1}{4^n (2n)! \sqrt{\pi}} \frac{H_{2n}^2(\sqrt{E/\omega + 1/2})}{\sqrt{\omega(E + \omega/2)}} e^{-E/\omega - 1/2} \tag{16}$$

These functions present a divergence at $E = -\omega/2$, while the zeros of $\rho_0(E, |2n, -\rangle)$ are determined by the zeros of $H_{2n}^2(\sqrt{E/\omega + 1/2})$. Notice further the normalization

$$\int_{-\omega/2}^{\infty} dE \rho_0(E, |2n, -\rangle) = 1. \tag{17}$$

We can now contrast and calibrate the numerical results at $\omega_0 \neq 0$ for the first six states of the subspace \tilde{S}_{+1} with the corresponding analytical expression (16), in Fig. 5. Clearly the qualitative structure is well tracked by our numerical procedure, setting aside the divergence of ρ_0 at $E = -\omega/2$. In particular, notice the number of nodes in the corresponding spectral functions. Moreover, in Fig. 6 we plot the ratio between the two quantities. Even if the polynomial trend of the truncated continued fraction can not track the exponential trend of (16), in a range of high energies for which the Hermite trend contributes mostly, we can notice a constant value which is due to the atomic term in the Hamiltonian (8) becoming progressively less relevant.

The Survival Probability of the vacuum state

The results of the previous section can be exploited for the determination of an important dynamical quantity: the survival probability, that is, the probability of finding the system in its initial state after a time evolution of interval t .

The connection between the spectral function $\rho(E, |\Psi\rangle)$ and the survival probability is given through the survival amplitude $A_{\Psi}(t) = \langle \Psi | U(t) | \Psi \rangle = \langle \Psi | e^{-iHt} | \Psi \rangle$ by Fourier transform,

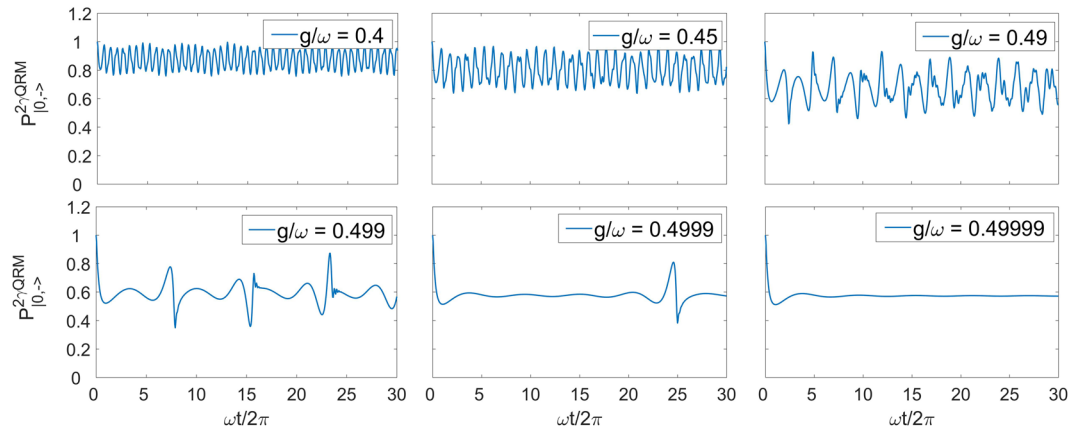


Figure 7. Survival Probability related to the vacuum state $|0, -\rangle$ of the 2γ QRM, approaching to the collapse point $g/\omega = 0.5$. The quantity is calculated through the spectral function of the state considered (see related section). For all cases $\omega_0 = 0.8\omega$.

$$\begin{aligned} \int dE e^{-iEt} \rho(E, |\Psi\rangle) &= \int dE e^{-iEt} \sum_{\lambda} |\langle \varepsilon_{\lambda} | \Psi \rangle|^2 \delta(E - E_{\lambda}) \\ &= \sum_{\lambda} |\langle \varepsilon_{\lambda} | \Psi \rangle|^2 e^{-iE_{\lambda}t} = \langle \Psi | e^{-iHt} | \Psi \rangle. \end{aligned} \tag{18}$$

That is,

$$P_{\Psi}(t) = |A_{\Psi}(t)|^2 = \left| \int dE e^{-iEt} \rho(E, |\Psi\rangle) \right|^2 \tag{19}$$

with the integration on the domain defined by $\rho(E, |\Psi\rangle)$.

Let us now focus on the vacuum state of the 2γ QRM. It is of interest since it can be prepared as the ground state in the decoupled or strong coupling regime ($g/\omega \ll 0.1$), and then adiabatically moved to larger couplings. In terms of the eigenenergies E_{λ} and the transition probabilities $|\langle \varepsilon_{\lambda} | 0, - \rangle|^2$, which can be derived from its spectral function, the survival probability of the vacuum state $|0, -\rangle$ can be written as:

$$P_{|0,-\rangle}(t) = \left| \sum_{\lambda} |\langle \varepsilon_{\lambda} | 0, - \rangle|^2 e^{-iE_{\lambda}t} \right|^2 \tag{20}$$

This connection provides us with a numerical technique to compute the survival probability, through numerical computation of the spectral function. The fact that we do not use matrix inversion, diagonalization, nor exponentiation in the process means that the point of the truncation can be much higher than what could be reasonably achieved with Fock space expansions for the survival probability. This numerical advantage allows us, in particular, an analysis of the survival probability for the 2γ QRM close to the collapse point $g = \omega/2$.

In Fig. 7 we report the numerical determination of the survival probability at different values of g/ω . Near the collapse point $g = \omega/2$ interference effects become predominant. This was to be expected from the spectral density depicted in Fig. 2, since the density of eigenstates means that small frequencies (small energy differences) will play a major role in the survival probability. Indeed the long time behaviour of the survival probability becomes flatter, as seen in the last graph of Fig. 7.

We also compute the survival probability for $g/\omega = 0.5$ at different values of ω_0 , as portrayed in Fig. 8. We again see that the survival probability for $|0, -\rangle$ presents a dominant constant value, dependent on the atomic parameter, after a short transient. This can be understood by looking at the form of the Survival Probability $P_{|0,-\rangle}(t)$ in terms of the spectral function,

$$P_{|0,-\rangle}(t) = \left| |\langle \varepsilon_0 | 0, - \rangle|^2 + \int_{-\omega/2}^{\infty} dE \rho(E, |0, -\rangle) e^{-iEt} \right|^2, \tag{21}$$

and application of the Riemann–Lebesgue lemma. Indeed, we know that $\rho(E, |0, -\rangle)$ is integrable - in fact, as pointed out above, it is normalized to 1. Therefore the Fourier transform above tends to zero at infinity. To be more precise, only the discrete part of the spectrum contributes to the long time behaviour,

$$\lim_{t \rightarrow \infty} P_{|0,-\rangle}(t) = |\langle \varepsilon_0 | 0, - \rangle|^4. \tag{22}$$

Moreover, the case $\omega_0 = 0$ (the blue line in Fig. 8) agrees with the analytical exact result from $\rho_0(E, |0, -\rangle)$:

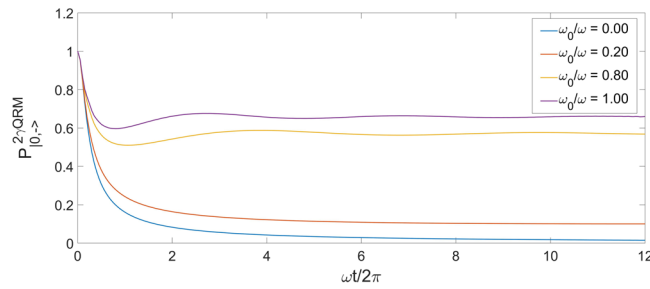


Figure 8. Survival Probability of the vacuum state $|0, -\rangle$ of the 2γ QRM in correspondence of the collapse point of the spectrum $g/\omega = 0.5$, at different values of the atomic frequency ω_0 . The case $\omega_0 = 0$ is consistent with the analytical result (23).

$$\begin{aligned}
 P_{|0,-\rangle}(t) &= \left| \int dE e^{-iEt} \rho_0(E, |0, -\rangle) \right|^2 \\
 &= \left| \frac{e^{i\omega t/2}}{\sqrt{\pi\omega}} \int_{-\omega/2}^{\infty} dE \frac{e^{-(1+i\omega t)(E/\omega + 1/2)}}{\sqrt{E/\omega + 1/2}} \right|^2 \\
 &= \frac{1}{\pi} \left| \int_{-\infty}^{+\infty} d\varepsilon e^{-(1+i\omega t)\varepsilon^2} \right|^2 = \frac{1}{\sqrt{1 + \omega^2 t^2}}.
 \end{aligned}
 \tag{23}$$

Notice the asymptotic $1/t$ behaviour, that is due to the $1/(E + \omega/2)^{1/2}$ divergence in the integrand.

As ω_0 grows, a discrete point will appear in the spectrum, and thus a constant term in the long time behaviour of the survival probability. The subleading term will be generically of form $1/t$, since the leading behaviour of the Fourier transform of the continuum part will be $1/t$ or faster decay.

Conclusions and Perspectives

In this work we have studied numerically spectral functions for the Two Photon Quantum Rabi Model (2γ QRM) and the corresponding survival probabilities. These two quantities are more readily amenable to numerical treatment than direct diagonalization of the Hamiltonian, as is shown by the much higher truncation numbers we can achieve in this approach.

Since there are indeed several proposals for quantum simulation implementation of the 2γ QRM^{11,30–32}, our improved numerical approach will prove beneficial for their analysis.

This improvement of numerics has allowed us to investigate further the collapse point, at which the spectrum becomes continuous. This is indeed the result recovered both from spectral functions and from survival probabilities.

As all numerics are suspect in the environment of a drastic structural change, such as the spectral collapse at hand, we have proposed an independent check by comparing spectral functions at the collapse point for the exactly solvable case with $\omega_0 = 0$, expressed in terms of Hermite polynomials, with those corresponding to $\omega_0 \neq 0$. The qualitative structure, in particular the number of modes and the large energy/short time behaviours, is maintained as expected, thus providing us with a calibration tool.

In particular we note that a signature of the collapse of the spectrum into a purely continuous one would be that all survival probabilities necessarily tend to zero. In the case at hand there is a remaining relevant discrete point in the spectrum, and the long time limit of the survival probability is a constant, determined by the projection of the initial state onto the corresponding proper eigenstate.

The direct measurement of such a phenomenon in the survival probability might not be immediately possible in the different platforms in which the 2γ QRM is a good description of the dynamics for some range of the parameters. However, there are alternatives to detect the spectral collapse, one of which we now put forward. Consider thus that there is another eigenstate of the full system which can be coupled to the discrete element of the $\tilde{\mathcal{S}}_{+1}$ subspace. In such a situation, the long term behaviour of the survival probability for any state in the $\tilde{\mathcal{S}}_{+1}$ subspace will be given by coherent Rabi oscillations, providing us with a target for detection.

Notice a very recent alternative proposal to investigate the spectral collapse, in this case for the 2γ QRM with full quadratic coupling, studying a two-time correlation for the output field in a driven system⁴³.

In summary, we have investigated further the rich phenomenology of the 2γ QRM, with emphasis on the numerically computable spectral functions and survival probability, and we suggest new avenues for the exploration of the spectral collapse.

Appendix A: The continued fraction form of the resolvent

In each subspace of defined four-parity Π_4 the rotated Hamiltonian \tilde{H} is tridiagonal in the basis of Fock states. For instance, the 2γ QRM Hamiltonian projected in the subspace of positive parity $\tilde{\mathcal{S}}_{+1}$ is (see Eq. (8)):

$$\tilde{H}_{+1} = \omega a^\dagger a + g(a^2 + (a^\dagger)^2) - \frac{1}{2}\omega_0 \cos\left(\frac{a^\dagger a}{2}\pi\right)
 \tag{24}$$

Since the elements $\langle 2n, - | \tilde{H}_{\pm 1} | 2m, - \rangle$ are non-zero only if $m = n, n \pm 1$, the matrix form of the projected Hamiltonian assumes a tridiagonal form in the basis $|2n, -\rangle$:

$$\tilde{H}_{\pm 1} = \begin{pmatrix} A_0 & R_1 & 0 & 0 & \dots \\ R_1 & A_1 & R_2 & 0 & \dots \\ 0 & R_2 & A_2 & R_3 & \dots \\ \vdots & & \ddots & \ddots & \ddots \end{pmatrix} \tag{25}$$

where $A_n = \langle 2n | \tilde{H}_{\pm 1} | 2n \rangle = 2n\omega - (-1)^n \omega_0/2$ and $R_n = \langle 2n | \tilde{H}_{\pm 1} | 2n - 2 \rangle = \langle 2n - 2 | \tilde{H}_{\pm 1} | 2n \rangle = g\sqrt{2n(2n - 1)}$.

As regards to the resolvent related to this Hamiltonian, $R_{\tilde{H}_{\pm 1}}(z) = (z - \tilde{H}_{\pm 1})^{-1}$, we can see that its diagonal elements $\langle 2n, - | R_{\tilde{H}_{\pm 1}}(z) | 2n, - \rangle$ can be expressed in a continued fraction form. If one is interested only in the first element $\langle 0, - | R_{\tilde{H}_{\pm 1}}(z) | 0, - \rangle$ the continued fraction form can be achieved also through the Recursive Projection Method⁴⁰. However, since it is a general property of the tridiagonal matrices one can exploit the iterative relation of tridiagonal matrix minors for the determination of a generic element of the resolvent⁴¹.

In this section we show how to obtain equation (13), namely the continued fraction form of the element $\langle n, \sigma | TR_{\tilde{H}} T^\dagger | n, \sigma \rangle$, with $|\Psi\rangle = T^\dagger |n, \sigma\rangle$ state belonging to any one of the four subspaces (7). We derive the expression for $|\Psi\rangle \equiv |2n, -\rangle \in \tilde{S}_{\pm 1}$. Since the form of the Hamiltonian \tilde{H} in any of the subspaces $\tilde{S}_{\pm 1, \pm i}$ is the same as (25), the derivation of the diagonal element of the resolvent does not change from the one in the subspace $\tilde{S}_{\pm 1}$.

From the theory of linear algebra the inverse of a square matrix Q is the matrix of elements $Q_{ij} = \Delta_{ij}/\det(Q)$, where $\Delta_{ij} = (-1)^{i+j} \det(M_{ij})$ is the (i, j) -cofactor and M_{ij} is the first minor, obtained by eliminating the i -th row and the j -th column. We use the following notation: D_0 as the determinant of $(z - \tilde{H}_{\pm 1})$, D_k as the corresponding determinant of the matrix resulting from eliminating the first k rows and k columns, and \tilde{D}_k as the determinant of the matrix given by the restriction to the first $k + 1$ rows and columns of the same matrix. So we have:

$$D_0 = \det(z - \tilde{H}_{\pm 1}) \tag{26a}$$

$$D_n = \det \begin{pmatrix} z - A_n & R_{n+1} & 0 & \dots \\ R_{n+1} & z - A_{n+1} & R_{n+2} & \dots \\ \vdots & \ddots & \ddots & \ddots \end{pmatrix} \tilde{D}_n = \det \begin{pmatrix} z - A_0 & R_1 & \dots \\ R_1 & z - A_1 & R_2 \\ \dots & \dots & \ddots & R_n \\ \dots & \dots & R_n & z - A_n \end{pmatrix} \tag{26b}$$

Since the sub-matrix obtained by removing the n -th row and n -th column of $(z - \tilde{H}_{\pm 1})$ has a block-tridiagonal form, applying the formula for the inverse matrix we have:

$$\langle 2n, - | (z - \tilde{H}_{\pm 1})^{-1} | 2n, - \rangle = \frac{\Delta_{nn}}{\det(z - \tilde{H}_{\pm 1})} = \frac{\tilde{D}_{n-1} D_{n+1}}{D_0} \tag{27}$$

Moreover, D_0 can be written in terms of \tilde{D}_{n-1} and D_{n+1} using the Laplace formula for the matrix determinant:

$$D_0 = \det(z - \tilde{H}_{\pm 1}) = (z - A_n) \tilde{D}_{n-1} D_{n+1} - R_{n+1}^2 \tilde{D}_{n-1} D_{n+2} - R_n^2 \tilde{D}_{n-2} D_{n+1} \tag{28}$$

Thus Eq. (27) takes the form:

$$\frac{\tilde{D}_{n-1} D_{n+1}}{D_0} = \frac{1}{(z - A_n) - R_{n+1}^2 D_{n+2}/D_{n+1} - R_n^2 \tilde{D}_{n-2}/\tilde{D}_{n-1}} \tag{29}$$

Using similar arguments a recursive formula for D_n/D_{n-1} and $\tilde{D}_n/\tilde{D}_{n+1}$ can be obtained:

$$\frac{D_n}{D_{n-1}} = \frac{1}{(z - A_{n-1}) - R_n^2 D_{n+1}/D_n} \quad \frac{\tilde{D}_n}{\tilde{D}_{n+1}} = \frac{1}{(z - A_{n+1}) - R_{n+1}^2 \tilde{D}_{n-1}/\tilde{D}_n} \tag{30}$$

Applying iteratively the two formulas (30) the two quantities D_n/D_{n-1} and $\tilde{D}_n/\tilde{D}_{n+1}$ can be expressed in a continued fraction and a finite continued fraction form respectively:

$$D_n/D_{n-1} = \frac{1}{(z - A_{n-1}) - \frac{R_n^2}{(z - A_n) - \frac{R_{n-1}^2}{(z - A_{n-1}) - \dots}} \tag{31a}$$

$$\tilde{D}_n/\tilde{D}_{n-1} = \frac{1}{(z - A_{n+1}) - \frac{R_{n+1}^2}{(z - A_n) - \dots \frac{R_1^2}{(z - A_0)}} \tag{31b}$$

Substituting them in equation (30) we obtain the continued fraction form of a diagonal element of the resolvent (13).

Appendix B: Convergence of the continued fraction expansion

We want to study the convergence of the continued fraction form we have given for the element $\langle 0, - |R_{\tilde{H}_{+1}}|0, - \rangle$ of the resolvent:

$$\langle 0, - |R_{\tilde{H}_{+1}}|0, - \rangle = \frac{1}{E - i\varepsilon + \omega_0/2} - \frac{2g^2}{E - i\varepsilon - 2\omega - \omega_0/2} - \frac{12g^2}{E - i\varepsilon - 4\omega + \omega_0/2} - \dots \tag{32}$$

Define for this case $a_0 = 1$, $a_n = g^2 2n(2n - 1)$ for $n \geq 1$, and $b_n = E - i\varepsilon - 2n\omega + (-1)^n \omega_0/2$ for $n \geq 0$. The continued fraction at hand is

$$\langle 0, - |R_{\tilde{H}_{+1}}|0, - \rangle = \frac{a_0}{b_0} - \frac{a_1}{b_1} \frac{a_2}{b_2} - \dots \tag{33}$$

This continued fraction can be written as

$$\frac{1/\omega}{\alpha_0} - \frac{1}{\alpha_1} - \frac{1}{\alpha_2} - \dots \tag{34}$$

with

$$\alpha_n = c_n b_n, \quad c_{n+1} = \frac{1}{a_{n+1} c_n}, \quad c_0 = 1/\omega.$$

The form of a_n makes it easy to provide an explicit form, namely

$$\alpha_{2n+1} = \frac{\omega b_{2n+1}}{a_{2n+1}} \prod_{l=1}^n \frac{a_{2l}}{a_{2l-1}} = \frac{\omega b_{2n+1}}{a_{2n+1}} \frac{\Gamma(\frac{1}{2})\Gamma(\frac{1}{4})}{\Gamma(\frac{3}{4})} \frac{\Gamma(n+1)\Gamma(n+\frac{3}{4})}{\Gamma(n+\frac{1}{2})\Gamma(n+\frac{1}{4})}.$$

$$\alpha_{2n} = \frac{b_{2n}}{\omega} \prod_{l=1}^n \frac{a_{2l-1}}{a_{2l}} = \frac{b_{2n}}{\omega} \frac{\Gamma(\frac{3}{4})}{\Gamma(\frac{1}{2})\Gamma(\frac{1}{4})} \frac{\Gamma(n+\frac{1}{2})\Gamma(n+\frac{1}{4})}{\Gamma(n+1)\Gamma(n+\frac{3}{4})}.$$

Notice that the coefficients α_n are adimensional. We can now use the Stirling approximation to obtain their asymptotic behaviour,

$$\alpha_{2n+1} = - \frac{4\omega^2}{16g^2} \frac{\Gamma(\frac{1}{2})\Gamma(\frac{1}{4})}{\Gamma(\frac{3}{4})} + O(n^{-1}),$$

$$\alpha_{2n} = -4 \frac{\Gamma(\frac{3}{4})}{\Gamma(\frac{1}{2})\Gamma(\frac{1}{4})} + O(n^{-1}).$$

We shall now see that, if $g^2 < \omega^2/4$, Pringsheim's sufficient convergence criterion allows us to conclude convergence for complex energy. In order to see this, consider rewriting the continued fraction as

$$\frac{1/\omega}{\alpha_0} - \frac{1}{\alpha_1} - \frac{1}{\alpha_2} - \dots = \frac{c/\omega}{\beta_0} - \frac{1}{\beta_1} - \frac{1}{\beta_2} - \dots, \tag{35}$$

for some real c . This is achieved by defining the coefficients β_n by $\beta_{2n+1} = \frac{\alpha_{2n+1}}{c}$ and $\beta_{2n} = c\alpha_{2n}$. Let $0 < \delta \ll 1$ be a small positive real number. Choose c as

$$c = - \frac{1}{2 + \delta} \frac{\omega^2}{4g^2} \frac{\Gamma(\frac{1}{2})\Gamma(\frac{1}{4})}{\Gamma(\frac{3}{4})}. \tag{36}$$

Then, asymptotically,

$$\beta_{2n+1} = 2 + \delta + O(n^{-1}),$$

$$\beta_{2n} = \frac{1}{2 + \delta} \frac{\omega^2}{g^2} + O(n^{-1}).$$

In order to fulfill, asymptotically, Pringsheim's criterion $|\beta_n| > 2$, we require

$$\frac{1}{2 + \delta} \frac{\omega^2}{g^2} > 2,$$

whence

$$g^2 < \frac{\omega^2}{2(2 + \delta)},$$

thus inside the normal region before the collapse.

The asymptotic convergence does not guarantee convergence of the resolvent if the energy is one of the real eigenvalues; it is enough for our purposes, though, since in order to determine the relevant spectral function we have to compute the limit of the imaginary part of the resolvent.

References

- Rabi, I. I. On the Process of Space Quantization. *Phys. Rev.* **49**, 324 (1936).
- Rabi, I. I. Space Quantization in a Gyration Magnetic Field. *Phys. Rev.* **51**, 652 (1937).
- Jaynes, E. T. & Cummings, F. W. Comparison of quantum and semi-classical radiation theories with application to beam maser. *Proc. IEEE* **51**, 89 (1963).
- You, J. Q. & Nori, F. Atomic physics and quantum optics using superconducting circuits. *Nature* **474**, 589–597 (2011).
- Georgescu, I. M., Ashhab, S. & Nori, F. Quantum simulation. *Rev. Mod. Phys.* **86**, 153 (2014).
- Romero G., Solano E. & Lamata L. *Quantum Simulations with Circuit Quantum Electrodynamics*, In: Angelakis, D. (ed.) *Quantum Simulations with Photons and Polaritons*. Quantum Science and Technology. Springer, Cham, pp 153–180 (2017).
- Pedernales, J. S. *et al.* Quantum Rabi Model with Trapped Ions. *Sci. Reps.* **5**, 15472 (2015).
- Forn-Daz, P. *et al.* Observation of the Bloch-Siegert Shift in a Qubit-Oscillator System in the Ultra-strong Coupling Regime. *Phys. Rev. Lett.* **105**, 237001 (2010).
- Niemczyk, T. *et al.* Circuit quantum electrodynamics in the ultrastrong-coupling regime. *Nat. Phys.* **6**, 772 (2010).
- Yoshihara, F. *et al.* Superconducting qubit-oscillator circuit beyond the ultrastrong-coupling regime. *Nature Physics* **13**, 44–47 (2017).
- Felicetti, S. *et al.* Spectral collapse via two-phonon interactions in trapped ions. *Phys. Rev. A* **92**, 033817 (2015).
- Casanova, J., Romero, G., Lizuain, I., Garca-Ripoll, J. J. & Solano, E. Deep Strong Coupling Regime of the Jaynes-Cummings model. *Phys. Rev. Lett.* **105**, 263603 (2010).
- Rossatto, D. Z., Villas-Bôas, C. J., Sanz, M. & Solano, E. Spectral Classification of Coupling Regimes in the Quantum Rabi Model. *Phys. Rev. A* **96**, 013849 (2017).
- Schweber, S. On the Application of Bargmann Hilbert Space to Dynamical Problems. *Ann. Phys., NY* **41**, 205 (1967).
- Braak, D. On the integrability of the Rabi Model. *Phys. Rev. Lett.* **107**, 100401 (2011).
- Braak, D. *Analytical Solutions of Basic Models in Quantum Optics*, In Anderssen, R. S. *et al.* (eds) *Proceeding of the Forum of Mathematics for Industry 2014*, Springer, NY (2015).
- Chen, Q., Wang, C., He, S., Liu, T. & Wang, K. Exact solvability of the quantum Rabi model using Bogoliubov operators. *Phys. Rev. A* **86**, 023822 (2012).
- Xie, Q., Zhong, H., Batchelor, M. T. & Lee, C. The quantum Rabi model: solution and dynamics. *J. Phys. A: Math. Theor.* **50**, 113001 (2017).
- Bargmann, V. On a Hilbert space of analytic functions and an associated integral transform part I. *Comm. Pure Appl. Math.* **14**, 197 (1961).
- Zhong, H., Xie, Q. T., Batchelor, M. & Lee, C. Analytical eigenstates for the quantum Rabi model. *J. Phys. A* **46**, 415302 (2013).
- Maciejewski, A. J., Przybylska, M. & Stachowiak, T. Full spectrum of the Rabi model. *Phys. Lett. A* **378**, 16 (2014).
- Sukumar, C. V. & Buck, B. Multi-photon generalization of the Jaynes and Cummings model. *Phys. Lett. A* **83**, 211 (1981).
- Davidovich, L., Raimond, J. M., Brune, M. & Haroche, S. Quantum Theory of a two-photon micromaser. *Phys. Rev. A* **36**, 3771 (1987).
- Puri, R. R. & Bullough, R. K. Quantum electrodynamics of an atom making two-photon transitions in an ideal cavity. *J. Opt. Soc. Am. B* **5**, 2021 (1988).
- Toor, A. H. & Zubairy, M. S. Validity of the effective Hamiltonian in the two-photon atom-field interaction. *Phys. Rev. A* **45**, 4951 (1992).
- Peng, J. S. & Li, G. X. Influence of the virtual-photon processes on the squeezing of light in the two-photon Jaynes-Cummings model. *Phys. Rev. A* **47**, 3167 (1993).
- Ng, K. M., Lo, C. F. & Liu, K. L. Exact eigenstates of the two-photon Jaynes and Cummings model with the counter rotating terms. *Eur. Phys. J. D* **6**, 119 (1999).
- Emary, C. & Bishop, R. F. Exact isolated solutions for the two-photon Quantum Rabi model. *J. Math. Phys.* **43**, 3916 (2002).
- Albert, V. V., Scholes, G. D. & Brumer, P. Symmetric rotating-wave approximation for the generalized single-mode spin-boson system. *Phys. Rev. A* **84**, 042110 (2011).
- Puebla, R., Hwang, M.-J., Casanova, J. & Plenio, M. B. Protected ultrastrong coupling regime of the two-photon quantum Rabi model with trapped ions. *Phys. Rev. A* **95**, 063844 (2017).
- Felicetti, S., Rossatto, D. Z., Rico, E., Solano, E. & Forn-Daz, P. Two-photon quantum Rabi model with superconducting circuits. *Phys. Rev. A* **97**, 013851 (2017).
- Schneeeweiss, P., Dareau, A. & Sayrin, C. Cold-atom based implementation of the quantum Rabi model, *arXiv:1706.07781* (2017).
- Travenec, I. Solvability of the two-photon Rabi Hamiltonian. *Phys. Rev. A* **85**, 043805 (2012).
- Travenec, I. Reply to Comment on “Solvability of the two-photon Rabi Hamiltonian”. *Phys. Rev. A* **91**, 037802 (2015).
- Zhang, Y. Z. On the solvability of the QRM and its two-photon and two-mode generalizations. *J. Math. Phys.* **54**, 102104 (2013).
- Zhang, Y. Z. Analytic solutions of 2-photon and two-mode Rabi models, *arXiv:1304.7827v2* (2014).
- Duan, L., Xie, Y., Braak, D. & Chen, Q. Two-photon Rabi model: analytic solutions and spectral collapse. *J. Phys. A: Math. Theor.* **49**, 464002 (2016).
- Metha, C. L., Roy, A. K. & Saxena, G. M. Eigenstates of two-photon annihilation operators. *Phys. Rev. A* **46**, 1565 (1992).
- Bentivegna, G. & Messina, A. Structure and properties of the ground state of a two-level system arbitrarily coupled to a boson mode including the counter-rotating terms. *Phys. Rev. A* **35**, 3313 (1987).
- Ziegler, K. Short note on the Rabi model. *J. Phys. A: Math. Theor.* **45**, 452001 (2012).
- Braak, D. Continued fraction and Rabi model. *J. Phys. A: Math. Theor.* **46**, 175301 (2013).

42. Swain, S. A continued fraction solution to a problem of a single atom interacting with a single radiation mode in the dipole approximation. *J. Phys. A: Math. Nucl. Gen.* **6**, 192 (1973).
43. Felicetti, S., Hwang, M. -J. & Le Boité, A. Ultrastrong coupling regime of non-dipolar light-matter interactions, *arXiv:1807.02434* (2018).

Acknowledgements

E.L. acknowledges fruitful discussions with D. Braak. I.L.E. and E.S. acknowledge funding from Spanish MINECO/FEDER FIS2015-69983-P and the Basque Government IT986-16.

Author Contributions

E.L. has performed the main calculations and numerical simulations and has been responsible together with I.E. for the writing of the paper. I.E. has contributed to theoretical calculations. A.M., A.N. and E.S. have contributed to the generation and development of the ideas and supervise the project throughout all stages.

Additional Information

Competing Interests: The authors declare no competing interests.

Publisher's note: Springer Nature remains neutral with regard to jurisdictional claims in published maps and institutional affiliations.



Open Access This article is licensed under a Creative Commons Attribution 4.0 International License, which permits use, sharing, adaptation, distribution and reproduction in any medium or format, as long as you give appropriate credit to the original author(s) and the source, provide a link to the Creative Commons license, and indicate if changes were made. The images or other third party material in this article are included in the article's Creative Commons license, unless indicated otherwise in a credit line to the material. If material is not included in the article's Creative Commons license and your intended use is not permitted by statutory regulation or exceeds the permitted use, you will need to obtain permission directly from the copyright holder. To view a copy of this license, visit <http://creativecommons.org/licenses/by/4.0/>.

© The Author(s) 2019